QM/MM Modeling the Ras–GAP Catalyzed Hydrolysis of Guanosine Triphosphate

Bella L. Grigorenko,[1] Alexander V. Nemukhin,[1]* Igor A. Topol,[2] Raul E. Cachau,[2] and Stanley K. Burt[2]
[1]*Department of Chemistry, M.V. Lomonosov Moscow State University, Moscow, Russian Federation*
[2]*Advanced Biomedical Computing Center, SAIC Frederick, National Cancer Institute at Frederick, Frederick, Maryland*

ABSTRACT **The mechanism of the hydrolysis reaction of guanosine triphosphate (GTP) by the protein complex Ras–GAP ($p21^{ras}$ – $p120^{GAP}$) has been modeled by the quantum mechanical—molecular mechanical (QM/MM) and ab initio quantum calculations. Initial geometry configurations have been prompted by atomic coordinates of a structural analog (PDBID:1WQ1). It is shown that the minimum energy reaction path is consistent with an assumption of two-step chemical transformations. At the first stage, a unified motion of Arg789 of GAP, Gln61, Thr35 of Ras, and the lytic water molecule results in a substantial spatial separation of the γ-phosphate group of GTP from the rest of the molecule (GDP). This phase of hydrolysis process proceeds through the low-barrier transition state TS1. At the second stage, Gln61 abstracts and releases protons within the subsystem including Gln61, the lytic water molecule and the γ-phosphate group of GTP through the corresponding transition state TS2. Direct quantum calculations show that, in this particular environment, the reaction GTP + H_2O → GDP + $H_2PO_4^-$ can proceed with reasonable activation barriers of less than 15 kcal/mol at every stage. This conclusion leads to a better understanding of the anticatalytic effect of cancer-causing mutations of Ras, which has been debated in recent years. Proteins 2005;60:495–503.** © 2005 Wiley-Liss, Inc.

Key words: G-proteins; Ras–GAP; GTP hydrolysis; QM/MM modeling

INTRODUCTION

Hydrolysis of guanosine triphosphate (GTP) by G-proteins, leading to guanosine diphosphate (GDP) and inorganic phosphate (Pi), constitutes one of the most important enzymatic reactions responsible for normal and tumorigenic cellular signal transduction.[1,2] Regular circulation between the GTP-bound ("ON") and GDP-bound ("OFF") states of human Ras proteins, stimulated by GTPase activating proteins (GAPs), may be suppressed by cancer-causing mutations at certain positions. The mechanism of this reaction and the role of mutations remain a subject of active debates.

The X-ray structure of the complex between human H-Ras ($p21^{ras}$) bound to GDP and GAP-334 ($p120^{GAP}$) in the presence of aluminum fluoride solved at a resolution 2.5 Å (PDBid: 1WQ1) by Scheffzek, Wittinghofer, and their colleagues[3] has been an important step in structural studies of GTP hydrolysis. This structure often serves as a source of initial atomic coordinates for modeling the enzymatic reactions for the Ras–GAP protein complex with trapped GTP. Throughout the paper we use the numbering of residues consistent with that of the 1WQ1 structure.

Several hypotheses have been formulated for the reaction mechanism,[4–14] surveying, in particular, the role of a specific residue, Gln61, from Ras. It is known that mutations of Gln61 reduce intrinsic GTPase activity of Ras.[15] Therefore this residue must play an important role in the reaction. It is believed[3] that upon binding to Ras, GAP reduces flexibility of the switches of the former, and a main-chain carbonyl group of Arg789 (the "arginine finger") of GAP promotes a proper orientation of Gln61 of Ras towards the lytic water molecule.

Molecular modeling may assist experimental findings and help to clarify the reaction mechanism; however, theoretical considerations of GTPase activated hydrolysis of GTP[4–10,16–20] resulted in a diversity of conclusions. In particular, the arguments have been provided in favor of the mechanism in which the GTP acts as a general base for its own hydrolysis, accepting both the proton and the hydroxyl ion from the breaking water molecule.[4–9] This scheme assumes two steps: a nucleophilic attack of the water molecule on the γ-phosphate and formation of a penta-coordinated intermediate, followed by breaking the P-O bond and generation of GDP and inorganic phosphate. The empirical valence bond (EVB) approach was employed to justify this concept and to estimate the activation barriers.[8,9] The parameters of potential functions used in these EVB calculations were calibrated for the reference hydrolysis reactions in water following the ab initio estimates of energy profiles and charge distributions for the molecular fragments involved in chemical transformations.[7] Then the reduction of the activation barrier in proteins relative to water was demonstrated in the EVB calculations.

Apart from consideration of the role of Gln61, an extensive discussion on the type of reaction mechanism (dissocia-

*Correspondence to: Alexander V. Nemukhin, Department of Chemistry, M.V. Lomonosov Moscow State University, Moscow, 119992, Russian Federation. E-mail: nemukhin@ncifcrf.gov or anem@lcc.chem.msu.ru

Received 23 September 2004; Revised 12 January 2005; Accepted 13 January 2005

Published online 19 May 2005 in Wiley InterScience (www.interscience.wiley.com). DOI: 10.1002/prot.20472

tive vs. associative) and the nature of the transition state for the GTP hydrolysis is presented in the literature. The paper of Sprang and colleagues[21] contains, probably, the most recent survey on the subject. The studies of kinetic isotope effects in Ras-catalyzed GTP hydrolysis (in the absence of GAP) described in Du et al.[21] provide evidence in favor of the dissociative mechanism with a "loose" transition state, although additional theoretical considerations are required for final conclusions. The most recent work from Warshel's group[9] simulated an S_N2 type associative mechanism, but did not exclude considerations of a more dissociative type of transition state.[8]

In this work, we explore the power of the hybrid quantum mechanical—molecular mechanical (QM/MM) methodology[22–24] for direct calculations of potential energy surfaces for the reacting system (GTP + H_2O) in the enzymatic (E) environment of the Ras–GAP protein complex, which allows us to analyze the reaction route as a flow between stationary points on the potential surfaces. In our previous paper,[20] describing primarily pure quantum chemical calculations for a cluster model of the Ras–GAP reaction center, the main emphasis was only on the first stage of the hydrolysis process leading to separation of the γ-phosphate group from GDP. The present contribution describes the entire reaction cycle at the QM/MM level of the theory. Quantum chemical calculations for small fragments of the reaction center included in this paper serve to confirm observations of the QM/MM treatment.

Comparison of computed energy profiles results in a conclusion that the low activation energy route is consistent with the mechanism, which suggests a direct involvement of Gln61 in proton transfer processes. This finding may help to elucidate the role of cancer-causing mutations of Ras at the Gln61 position.

SIMULATIONS

Application of the hybrid QM/MM technique implies partitioning of the entire molecular system into two parts, specified by the researcher. In the QM subsystem, the energy and forces acting on the atoms are computed according to quantum mechanical equations, while the atoms within the MM subsystem interact between themselves following the classical rules with the selected set of force-field parameters. The simulations described in this work have been performed by using our QM/MM realization[25–28] based on the effective fragment potential theory.[29] The essential feature of this flexible effective fragment QM/MM technique is that the coupling of QM and MM subsystems is treated at ab initio level, while all empirical parameters are contained entirely in the MM part. Each effective fragment comprising a few MM atoms interacts with the QM part, and polarization of the electron density of the quantum subsystem due to effects of the MM part is taken into account. All parameters of effective fragment potentials are obtained in preliminary ab initio calculations and are not subject to changes from one application to another. The computer program created on the base of the GAMESS[30] (more specifically, PC GAMESS[31]) quantum chemistry package and molecular modeling system TINKER[32] allows us to scan portions of composite QM/MM potential energy surface and locate stationary points on the surface.

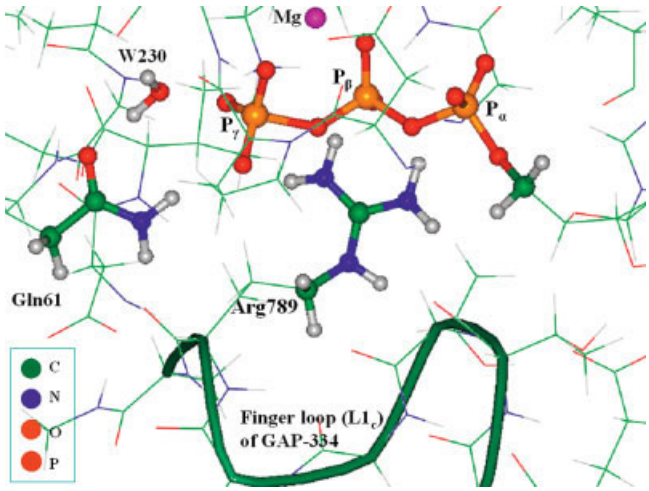

Fig. 1. The quantum subsystem (the ball and stick representation) and part of the MM subsystem (lines) in the vicinity of the reaction center. [Color figure can be viewed in the online issue, which is available at www.interscience.wiley.com.]

Figure 1 illustrates the appointed partitioning the system into QM and MM parts in an immediate vicinity of the reaction center. The atoms shown in the ball and stick representation refer to the QM subsystem (the closing, or "link" atoms are not exhibited in Fig. 1). The phosphate groups of GTP and the lytic water molecule, that is, the primary reagents, are necessarily included in the quantum region. Ionized magnesium (Mg^{2+}) and a fraction of the side chain of protonated Arg789 are the charged species close to the reagents, which must be important at least due to their electrostatic influence.

The role of another charged species in the close proximity to the reaction center, that is, the side chain of protonated Lys16 from Ras, has been debated in the literature.[8,16,17] In preliminary stages of our simulations we also included it in the quantum domain; however, we could not confirm an involvement of Lys16 in the key chemical transformations.[16,17] Therefore, in subsequent calculations we replaced the side chain of protonated Lys16 by effective fragments in the MM subsystem. Finally, the major part of the side chain of Gln61 was inserted to the QM part. In total, 43 atoms constituted the quantum subsystem. A large fraction of the protein complex Ras–GAP was taken into account as the MM part. More specifically, 1622 atoms from the protein complex within approximately 20 Å distance from the P_γ atom of GTP were included to the MM subsystem subdivided to 488 effective fragments. Part of the MM domain shown in Figure 1 is designated by lines. In particular, the important "finger loop" ($L1_c$) from GAP was considered explicitly. Most of the MM subsystem referred to the Ras protein. In total, 14 negatively charged residues (Asp: 30, 33, 38, 57, 92, 782, 789; Glu: 31, 37, 63, 143, 781, 783, 950) and 14 positively charged ones (Lys: 16, 88, 117, 147, 935,

949; Arg: 41, 68, 97, 149, 749, 789, 894, 903) were considered explicitly. The total charge of the quantum subsystem used in simulations was −1.

The search of minimum energy points on the composite QM/MM potential energy surface was performed as unconstrained minimization of coordinates of atoms in the QM subsystem and positions of effective fragments in the MM subsystem. Positions of remote effective fragments far away from the reaction center were not optimized. Consideration of saddle points on the potential surface connecting minimum energy configurations required sequences of constrained minimizations for an assumed reaction coordinate.

Geometry optimizations were carried out by using the Hartree-Fock approach in the QM part. The polarized "LANL2DZ(d,p) ECP" basis set (and the corresponding pseudopotential for phosphorus)[33] was used for all atoms except magnesium. For the latter, the standard 6–31 basis set was employed. In preliminary calculations we showed that such an approach provide the same or even better quality that conventional 6-31 + G(d,p) sets for all-electron ab initio calculations with phosphates. In the MM part, the AMBER[34] set of force field parameters was applied.

Standard quantum chemistry calculations of the equilibrium geometry configurations and saddle points on potential energy surfaces for smaller portions of the entire molecular system were carried out by using Gaussian98[35] program.

RESULTS

Starting from the coordinates of the 1WQ1 structure, we constructed the model molecular complex with the authentic GTP species trapped inside the proteins, selected a fraction of the system, as described above, and performed QM/MM unconstrained optimization of geometry parameters. Such procedure led us to the configuration, comprising GTP, lytic water molecule and enzyme (GTP + H_2O + E), which will be referred to as "Reagents."

Consistent with the conclusions from experimental kinetic studies,[36] calculations show that the hydrolysis reaction starts by an in-line nucleophilic attack of water molecule on the γ-phosphate group of GTP leading to stereochemical inversion of its configuration. The corresponding transition state should involve the γ-phosphate adopting a trigonal bipyramidal arrangement with the axial coordination sites being occupied by oxygens from the β-phosphate and lytic water molecule.[10] In simulations, we located the geometry configuration on the top of potential barrier, which was characterized by a planar arrangement of the $P(\gamma)O_3$ molecular group undergoing inversion. Such configurations, noted below as "TS1," was located as a result of the search of minimum energy path along two coordinates: the distance R1 between the oxygen atom of the lytic water molecule and the P_γ atom, and the distance R2 between P_γ and the bridging $O(P_\beta)$ atom bound to P_β. Descent from this point to the entrance valley led to the "Reagents" configuration. In the crystal structure, the arrangement in the active site of 1WQ1 with the GTP analog is assumed[3] to mimic this transition state, since a planar AlF_3 substitute replaces an intrinsic $P(\gamma)O_3$ group in the crystal.

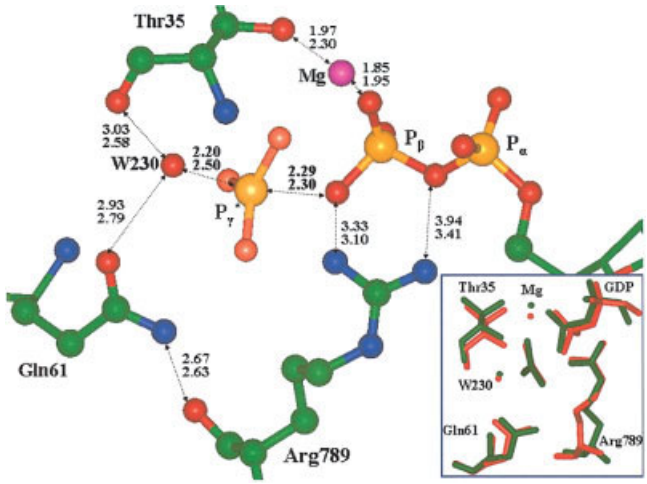

Fig. 2. Configuration of selected heavy atoms from the 1WQ1 structure and configuration on the top of the first barrier (TS1) on the QM/MM potential surface. The terminal group of guanisine phosphate (AlF_3 in 1WQ1 or $P(\gamma)O_3$ in simulations) is designated as the P_γ* group. Upper values of interatomic distances (Å) refer to 1WQ1, lower values correspond to calculation results. The inset shows superposition of both structures: green, experimental; red, theoretical. [Color figure can be viewed in the online issue, which is available at www.interscience.wiley.com.]

In Figure 2 we compare the geometry configuration of heavy atoms for the reaction site in the 1WQ1 structure to that at the top of the barrier on the computed potential energy surface. It would not be practical to expect a complete agreement between geometry parameters in the crystal with the GTP analog and in simulations. However, remarkable similarity in experimental and theoretical structures of the molecular fragments around the reacting center is notable.

Descent from the configuration "TS1" to the exit valley led to the minimum energy point on the potential energy surface denoted below as "Intermediate" (Fig. 3). This is a structure with a broken $P_\gamma - O(P_\beta)$ bond (R2 = 3.12 Å), and one can say that the GTP molecule has already dissociated at this stage. However, the lytic water molecule remains unaltered, and inorganic phosphate has not been formed.

The role of Arg789 from GAP seems, in particular, to assist in positioning Ras residue Gln61. In turn, Gln61 and Thr35 orient the attacking water molecule (W230) by their carbonyl groups. A consolidated action of Arg789, Gln61, Thr35 and the lytic water molecule results in a substantial spatial separation of the γ-phosphate group of GTP from the rest of the molecule. The distances R2 between P_γ and $O(P_\beta)$ are essentially the same in the crystal (2.29 Å) and at the top of the potential barrier (2.30 Å). In simulations, Arg789 approaches closer to the bridged oxygen atoms of β- and α-phosphate groups than in the crystal structure, while the distances between Arg789 and Gln61 in crystal and in simulations are practically the same. To complete the reaction, one must find the route from this "Intermedi-

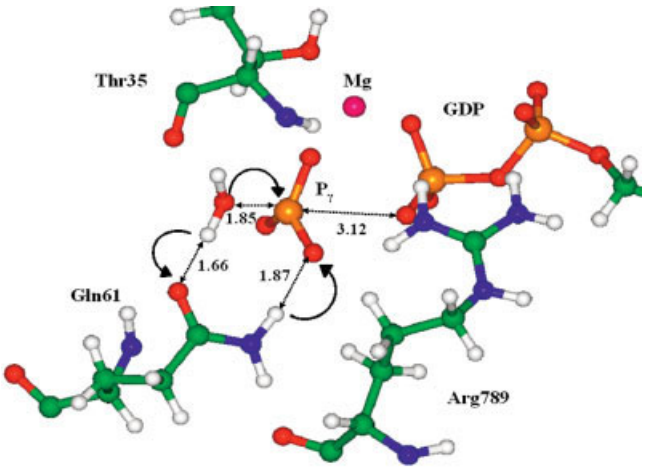

Fig. 3. Computed equilibrium geometry configuration for the "Intermediate" structure showing selected distances in Å. Arrows indicate directions of possible rearrangements to form the inorganic phosphate $H_2PO_4^-$. [Color figure can be viewed in the online issue, which is available at www.interscience.wiley.com.]

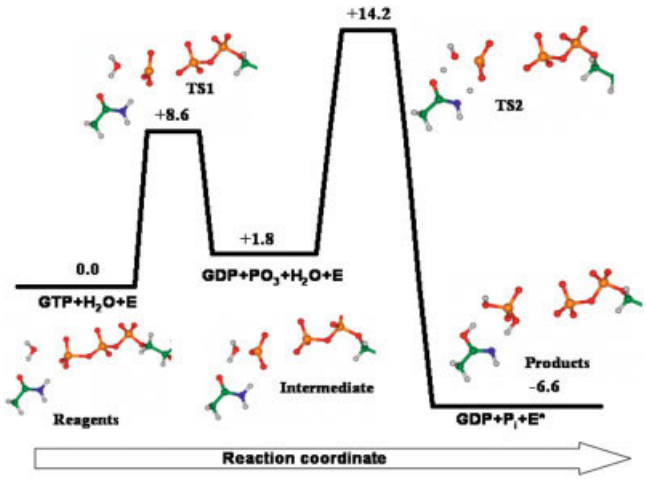

Fig. 4. Schematic energy diagram (in kcal/mol) along the reaction pathway constructed by the results of QM/MM calculations. The origin of energy refers to the enzyme–substrate complex GTP + H_2O + E. The outward minimum to the right refers to the reaction products GTP + Pi + E*, where E* designates that Gln61 stands in the higher energy tautomeric form. [Color figure can be viewed in the online issue, which is available at www.interscience.wiley.com.]

ate" structure to "Products" GDP + $H_2PO_4^-$, apparently through a saddle point on the potential energy surface, corresponding to the second transition state, "TS2." If kinetic measurements,[36] X-ray,[3] and vibrational spectroscopy[21] studies provide certain hints for the first stage, no helpful tips from experiments can be explored for the second stage. Observation of the computed equilibrium geometry configuration for the "Intermediate" structure (Fig. 3) suggests possible reaction flow towards formation of inorganic phosphate. The separated γ-phosphate group, Gln61 and lytic water are in perfect position for a concerted proton transfer with an active participation of Gln61, as shown in arrows in Figure 3.

A careful search of the minimum energy path along coordinates of proton transfers O(Water)-H-O(Gln61) and N(Gln61)-H-O(P_γ) resulted in both configurations "TS2" and "Products." The latter one was obtained under an unconstrained minimization of all variable geometry parameters in the QM/MM system. The configuration at the saddle point "TS2" connected the points "Intermediate" and "Products" on the potential surface. Figure 4 presents the computed energy profile for the entire hydrolysis reaction. The relative energies on the graph correspond to the results of SCF/LANL2DZ(d,p) calculations in the QM part and the use of the AMBER parameters in the MM part (the pure MM-energies are not included). The insets to Figure 4 show arrangements of most critical molecular groups.

The most important conclusion that may be drawn from these simulations is that the computed energy values seem to be very reasonable for biochemical reactions. It is exothermic, and the reaction energy is estimated as 6.5 kcal/mol. The highest energy barrier is on the route from "Intermediate" to "Products" amounting to 12.4 kcal/mol. To verify whether this conclusion depends on the computational protocol we present the results of ab initio quantum chemical calculations for a simplified model system com-

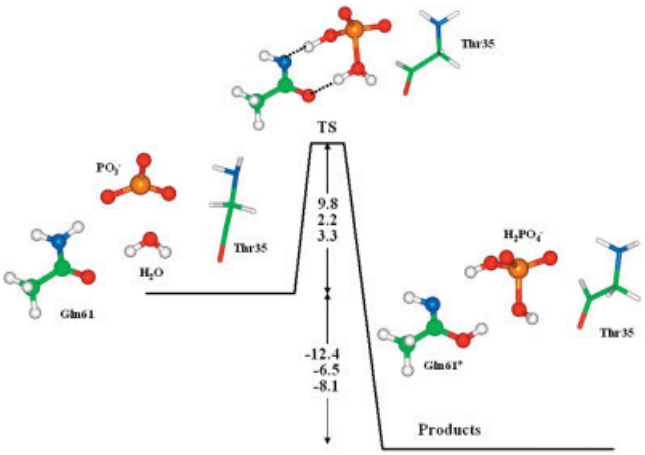

Fig. 5. Schematic energy diagram along the reaction pathway from the "Intermediate" to "Products" structures, modeled by the results of pure quantum chemical calculations for the simplified 25-atomic fragment of the entire system in vacuum. Relative energy values (kcal/mol) correspond to the following modes of calculations: SCF/6-31 + G(d,p) (top) B3LYP/6-31 + G(d,p) (middle), MP2/6-311 + G(d,p) (bottom). [Color figure can be viewed in the online issue, which is available at www.interscience.wiley.com.]

posed of critical parts of Gln and Thr residues, water molecule and the PO_3^- group (Fig. 5). The system in the left inset in Figure 5 mimics the "Intermediate" structure. It corresponds to the true minimum energy point on the 25-atomic potential energy surface with all real vibrational frequencies. The carbonyl groups of "Gln61" and "Thr35" orient water molecule with respect to the PO_3^- group by hydrogen bonds as in the parent system. The system in the right inset in Figure 5 mimics the "Products." It also refers to the true minimum on this potential surface with all real vibrational frequencies. The transition state (TS) structure was located as a point with a

single imaginary frequency. The energy values shown in Figure 5 correspond to the following modes of calculations: SCF/6-31 + G(d,p) (top), B3LYP/6-31 + G(d,p) (middle), MP2/6-311 + G(d,p) (bottom). In every case a complete geometry optimization was performed and vibrational frequencies were computed. These results provide important arguments favoring conclusions of the QM/MM calculations for the large molecular system, although the change in interaction with the protein upon change of the ab initio method used may affect the conclusions obtained by these gas phase studies. They prove (in accordance with usual quantum chemical practice) that the energy barrier for the critical second stage of hydrolysis computed by using the Hartree-Fock method in the QM part (8.6 kcal/mol from "Reagents" or 12.4 kcal/mol from "Intermediate" configurations) should not increase if electronic correlation effects are taken into account.

Clearly, the assumed reaction path leading to formation of inorganic phosphate from water and PO_3^- with a direct involvement of Gln in proton transfers must be a low barrier process and may occur in the Ras–GAP hydrolysis of GTP. The remaining concern to be discussed refers to the observation that in such a development the enzyme appears at the end of the reaction in an altered state compared to the initial status. Namely, the Gln61 residue turns out to be in a higher energy tautomeric imino form (Figs. 3–5). However, this observation does not oppose the suggested mechanism for the following reasons. While activation barriers for imino-amino tautomerization of molecules of formamide type may be high enough in the gas phase, the presence of few water molecules assist in drastic reduction of such barrier through formation of proton transfer routes along hydrogen bonds (see, for example, recent articles by Fu et al.[37] and Markova and Enchev[38]). We carried out quantum chemistry calculations for the reaction $HN = C(CH_3)OH \rightarrow NH_2C(CH_3)O$, mediated by one or two water molecules, by using the B3LYP/6-31 + G(d,p) and MP2/6-311 + G(d,p) methods. These results confirm that: (1) the potential barriers on the corresponding potential energy surfaces should not exceed 13 kcal/mol; (2) such barriers should further decrease when more water molecules are involved in the hydrogen bond chains; (3) the barriers decrease when dielectric continuum model (with $\varepsilon = 4$) is applied to model effects of a protein environment. In turn, molecular dynamics simulations for the Ras–GAP/GTP complex carried out by us show that the dissociation of the P_γ–$O(P_\beta)$ bond may lead to changes of the active site and to the leakage of external water close to the reacting species.[20] Therefore, restoring the amino tautomeric status of Gln61 cannot be a bottleneck for the entire process.

Numerical mutation experiments provide additional support to the mechanism under discussion. As estimated by Glennon, Villa, and Warshel,[8] the measured[39] reduction of the rate constant of GTP hydrolysis by the Ras–NF1 protein complex (relative to Ras–GAP) due to mutations of Arg may be converted to the corresponding increase of activation energy by ~ 4.5 kcal/mol. Reduction of the rate constant of the same order was also observed experimentally in the Rho–GAP complex by mutating Arg by Ala.[40] We repeated QM/MM simulations of the entire catalytic cycle for the model system, in which Arg789 was replaced by Leu at position 789, assuming that the entire structure of the protein complex did not change dramatically upon such mutation. In Figure 6 we compare the energy diagrams for the system with Arg789 (the same as in Fig. 4) and for the mutated model system, in which Arg789 is replaced by Leu. The effect of increasing potential barriers because of mutation is clearly seen. If we compare barriers of the second stage leading to "Products" referenced to the corresponding "Intermediate" levels, then their difference (16.7–12.4) turns out to be very close to the estimated value of 4.5 kcal/mol in the article by Glennon, Villa, and Warshel.[8] Analysis of geometry configurations referring to the respective "Intermediate" structures (insets in Fig. 6) clarifies the reasons for higher barrier in the mutated system. In the case of Leu the $P(\gamma)O_3^-$ stands closer to GDP, the lytic water molecule is farther from $P(\gamma)O_3^-$ and from Gln61, than in the initial system with Arg. Therefore, the proton transfers of the second stage should be easier when Arg is present in the protein complex.

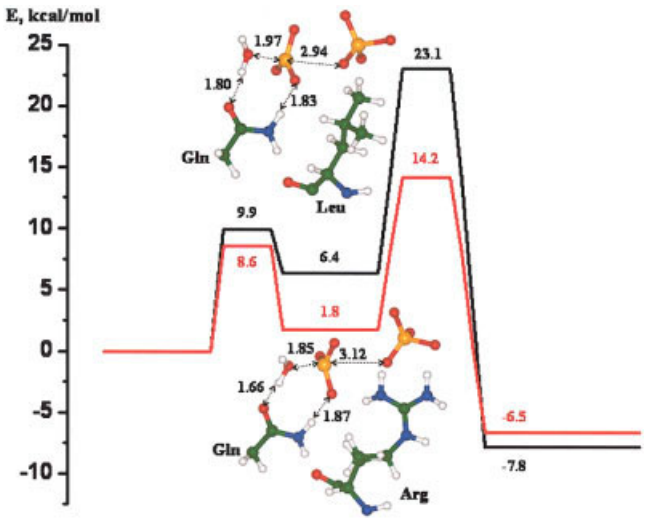

Fig. 6. Comparison of energy diagrams for the system with Arg789 (red) and the mutated model system, in which Arg789 is replaced by Leu (black). Geometry configurations in insets (distances are given in Å) refer to the corresponding "Intermediate" structures. [Color figure can be viewed in the online issue, which is available at www.interscience.wiley.com.]

DISCUSSION

A majority of studies on the GTP hydrolysis by Ras and Ras–GAP underline an important role of Gln61 in this reaction. The undoubted point of view is that this residue provides an appropriate position for the lytic water molecule. The potential mechanism of the GTP hydrolysis by G-proteins, according to which Gln abstracts a proton from the attacking water molecule while simultaneously donates a proton to a γ-phosphate oxygen, has been suspected (as one of the alternatives) by Sondek, Sigler, and colleagues when considering the crystal structure of trans-

ducin α · GDP activated with aluminum fluoride at 1.7 Å resolution.[41]

However, such a scenario was disputed later[6,10] on the basis that formation of the imino form of Gln should be "highly unfavorable ($\Delta G_{taut} \approx 10$ kcal/mol) so that the proton transfer or active site would need to provide an enormous amount of compensating transition state stabilization."[10] Schweins and Warshel[6] performed more detailed analysis of this tautomer-based catalytic mechanism. They estimated the energy expenses for the proton shuttle mechanism by using an indirect way, that is, via edges of the relevant rectangular energy diagram instead of the center region, and predicted the activation barrier higher than 50 kcal/mol. The key references were given to ab initio calculations of energy differences between tautomers of formamide in aqueous solution and to the results of empirical valence bond calculations.[6] These considerations, as well as those in the original paper,[41] assume that the reaction proceeds through the *pentavalent intermediate at the P_γ atom*. However, this is not the case for the mechanism presented in our work.

In accord with the expectations presented in Schweins and Warshel[6] and Maegley et al.[10] our direct calculations of the energy profile for the proton shuttle mechanism with participation of Gln61, *before* the γ-phosphate is stereochemically inverted and separated from GDP, actually predict "enormous" energy expenses along such a route (close to the estimates of Schweins and Warshel[6]). The significance of the first stage of the process (Reagents → TS1 → Intermediate), discussed in our work, is that it creates a new reactive species, PO_3^-. The results of our quantum calculations for the reaction $HN = C(CH_3)OH \rightarrow NH_2C(CH_3)O$ described in the previous section are, of course, consistent with the observation that the energy of Gln + H_2O should be lower than that of Gln* + H_2O by about 10 kcal/mol. However, as shown in Figure 4 (and even more clearly in Fig. 5), upon inclusion of PO_3^- in the system, the energy balance reverses: the energy of Gln + H_2O + PO_3^- is higher than that of Gln* + $H_2PO_4^-$. In turn, occurrence of the first stage, leading to separation of γ-phosphate is strongly supported by the present QM/MM calculations and previous ab initio quantum calculations for the cluster model.[20] In the latter case, a low-energy transition state structure with a single imaginary frequency, apparently referred to the break of the P_γ–$O(P_\beta)$ bond was located. These calculation results are also consistent with the most recent experimental supports[21] of the "loose" transition state (TS1 in our mechanism).

Another argument of Schweins and Warshel[6] formulated against the Gln61 as a proton shuttle mechanism was that in case of proton transfer being "a part of the transition state and hence also part of the rate-limiting step" one would expect a large solvent isotope effect, what was not observed experimentally.[6] Although exhaust theoretical simulations of the solvent isotope effect would require estimates of multiple factors, including tunneling corrections, we only evaluated contributions to the free energies of activation for a simplified model system. We considered the reaction illustrated in Figure 5 and performed the B3LYP/6-31 + G(d,p) calculations for the reagent and saddle point configurations with a different choice of hydrogen species. When hydrogen atoms in the water molecule were replaced by D ($H_2O \rightarrow D_2O$), the activation energy increased by 0.32 kcal/mol. Only in the case, when in addition to water, deuteration of both hydrogens in the amine group of Gln61 was performed, the corresponding increase of the barrier amounted to 1.14 kcal/mol, which could lead to a noticeable isotope effect.

As already mentioned in Introduction, the phosphate-as-a-basis mechanism in which GTP acts as a general base for its own hydrolysis, accepting the proton and the hydroxyl anion from the breaking water molecule, has gained a support in previous studies.[4–9] In this work we applied the same QM/MM approach as described in previous Sections to estimate the energy profile for a related mechanism. We started simulations from the "Intermediate" structure shown in Figure 3, that is, from the point GDP + PO_3 + H_2O + E in Figure 4. The computed energy diagram (Fig.7) must be compared to the right-side moiety of Figure 4 showing the barrier height 12.4 kcal/mol and the energy of products −8.4 kcal/mol relative to the starting point. The minimum energy path was constructed by using the following strategy. First, we created a series of points on the potential energy surface by imposing two constraints: the distance between oxygen O_w from water and phosphorus P_γ, and the distance between hydrogen H_{W2} from water and oxygen $O_{\gamma 1}$ from γ-phosphate. All other geometry parameters were optimized. Second, we relaxed the restrictions and only the distance H_{W2}-$O_{\gamma 1}$ was considered as a constraint in minimization. As a result we found the point ($R(H_{W2} - O_{\gamma 1}) = 1.30$ Å) on the energy surface corresponding to the top of the barrier. The corresponding structure is illustrated in the upper panel in Figure 7. Unconstrained minimization from this point towards the product valley led us to the structure shown in the right panel in Figure 7, in which the molecule of inorganic phosphate P_i could be identified. Geometry configuration of the latter (with the P–O distances 1.51 and 1.49 Å, and P–OH distances 1.64 and 1.57 Å) correlates fairly well to the structure of $H_2PO_4^-$ reported by Florian and Warshel by the results of their ab initio calculations (Fig. 5 of Florian and Warshel[7]). Also, our computed partial charges on atoms of P_i resemble those reported there. The energy difference between the starting point and the barrier height is estimated as 31.6 kcal/mol for this mechanism. Such value is considerably higher than the estimate 12.4 kcal/mol for the mechanism with a direct involvement of Gln61 in the chemical transformations leading to the products (Fig. 4).

One can argue that the Hartree-Fock approximation introduces errors in the computed energy values, and electron correlation effects may considerably reduce the activation energies. To estimate the role of electron correlation, we carried out single point calculations by using the second order Moller-Plessett perturbation theory (MP2) for the geometry configurations optimized at the Hartree-Fock level. As expected the barrier height decreased (26.7

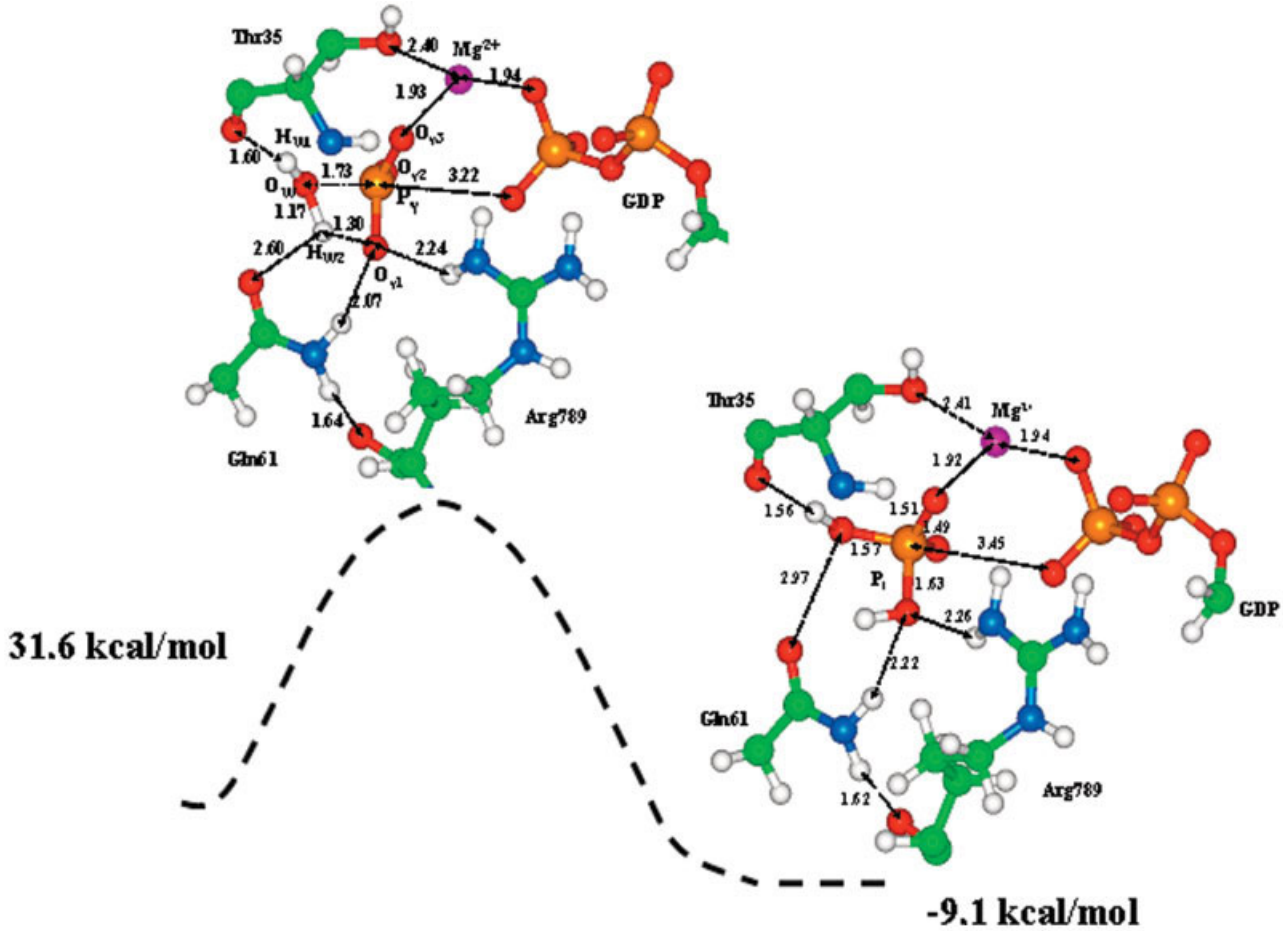

Fig. 7. Configurations of the active sites corresponding to the transition state and product structures for the phosphate-as-a-basis mechanism through the oxygen atom $O_{\gamma 1}$ of γ-phosphate. The energies are given with respect to the "Intermediate" structure shown in Figure 3, that is, with respect to the point GDP + PO_3 + H_2O + E in Figure 4. The profile in the present figure should be compared to the right-side moiety of Figure 4 showing the barrier height 12.4 kcal/mol and the energy of products −8.4 kcal/mol. Interatomic distances are given in Å. [Color figure can be viewed in the online issue, which is available at www.interscience.wiley.com.]

kcal/mol compared to 31.6 kcal/mol), but remained still too high for the enzymatic reaction. Moreover, the use of the same procedure (single point MP2 estimates at the Hartree-Fock geometry configurations) decreases the barrier heights for the competitive mechanism as well.

The same energy estimates and the same considerations hold for other possible channels of the phosphate-as-a-base mechanism, namely, through the oxygen atoms $O_{\gamma 2}$ and $O_{\gamma 3}$ of γ-phosphate. In those cases, the phosphate oxygens are bound to the protons from Lys16 and Gly60, or to Mg^{2+} and the proton from Thr35, respectively.

Other quantum chemical calculations for the direct attack of the water molecule on the γ-phosphate in a related molecular models have been described in our previous paper.[20] It that study, the energy profiles for a direct attack of water molecule on the phosphate has been computed by using the density functional theory and QM/MM methods. All calculations predicted too-high activation energies (about 40 kcal/mol) for such a single-step process.

Although reliability of the QM/MM approach applied in this work was tested in many challenging tests[27] and used before for successful simulations of the serine protease catalytic cycle[28] and for modeling chemical reactions in water,[42,43] its direct application to biological problems still requires certain caution. This methodology is based on the analysis of stationary points on the potential energy surface, but not of the free energy surface. As any quantum chemical calculation procedure, these simulations may be dependent on such details as basis set and treatment of electron correlation effects. An additional limitation presents a restriction by single starting conformation of the protein (consistent with the 1WQ1 structure) as a source of initial atomic coordinates for QM/MM calculations. In future work, we are planning to improve these limitations and also to perform calculations for the reference reaction in water, which will provide suitable calibration of the method; however, even at the present level of the theory the simulations raise a possibility of chemical involvement of Gln61 in the mechanism of action of Ras–GAP.

CONCLUSIONS

Present QM/MM and ab initio quantum chemical simulations result in that conclusion that hydrolysis of GTP by the Ras–GAP protein complex is a two-stage process.

At the first stage, a unified action of Arg789 of GAP, Gln61, Thr35 of Ras, and the lytic water molecule leads to a substantial spatial separation of the γ-phosphate of GTP from the rest of the molecule. At the second stage, inorganic phosphate $H_2PO_4^-$ is formed from water and the separated PO_3^- group with an active participation of Gln61 in proton transfers.

Although a concerted proton transfer through Gln61 from Ras in a phosphate-as-a-base mechanism has been suspected before,[41] principally new features have been revealed in our simulations. The first stage of dissociation of GTP across the P_γ–$O(P_\beta)$ bond is necessary to facilitate subsequent proton transfers. QM/MM and ab initio calculations predict that in this particular environment the reaction proceeds towards guanosine diphosphate (GDP) and inorganic phosphate with activation barriers of less than 15 kcal/mol at every stage.

These results help to develop a better understanding of the anticatalytic effect of cancer-causing mutations of Ras at position 61; a topic which has been debated in recent years. Der, Finkel, and Cooper, who found that 17 different mutant proteins at codon 61 of the human ras^H gene displayed "reduced rates of GTP hydrolysis, eightfold to 10-fold lower than the normal protein,"[15] suggested two explanations of their observations: either the normal amino acid (glutamine) is directly involved in the hydrolysis of GTP; or the amino acid 61 (along with Gly12) represent strong conformation-determining regions of Ras. Our calculations provide strong support to the direct involvement of Gln61 in key chemical transformations upon GTP hydrolysis by Ras–GAP.

ACKNOWLEDGMENTS

We thank Prof. A. Warshel for stimulating discussions on the subject and for making available the results of his work[9] prior the publication. The research described in this publication was made possible in part by Award No. RC1-2350-MO-02 of the U.S. Civilian Research and Development Foundation for the Independent States of Former Soviet Union (CRDF). This work is also supported in part by the grants from the Russian Foundation for Basic Researches (04-03-32008). We thank the staff and administration of the Advanced Biomedical Computing Center for their support of this project. This project has been funded in whole or in part with Federal funds from the National Cancer Institute, National Institutes of Health, under Contract No. NO1-CO-12400. The content of this publication does not necessarily reflect the views or policies of the Department of Health and Human Services, nor does mention of trade names, commercial products, or organization imply endorsement by the U.S. Government.

REFERENCES

1. Bourne HR, Sanders DA, McCormick F. The GTPase superfamily: conserved structure and molecular mechanism. Nature 1991;349:117–127.
2. Sprang SR. G protein mechanisms: Insight from structural analysis. Annu Rev Biochem 1997;66:639–678.
3. Scheffzek K, Ahmadian MR, Kabsch W, Wiesmüller L, Lautwein A, Schmitz F, Wittinghofer A. The Ras-RasGAP complex: structural basis for GTPase activation and its loss in oncogenic Ras mutants. Science 1997;277:333–338.
4. Langen R, Schweins T, Warshel A. On the mechanism of guanosine triphosphate hydrolysis in ras p21 proteins. Biochemistry 1992;31:8691–8696.
5. Schweins T, Langen R, Warshel A. Why have mutagenesis studies not located the general base in ras p21? Nat Struct Biol 1994;1:476–484.
6. Schweins T, Warshel A. Mechanistic analysis of the observed linear free energy relationships in $p21^{ras}$ and related systems. Biochemistry 1996;35:14232–14243.
7. Florian J, Warshel A. Phosphate ester hydrolysis in aqueous solution: associative versus dissociative mechanisms. J Phys Chem B 1998;102:719–734.
8. Glennon TM, Villa J, Warshel A. How does GAP catalyze the GTP reaction of Ras?: a computer simulation study. Biochemistry 2000;39:9641–9651.
9. Shurki A, Warshel A. Why does the Ras switch "break" by oncogenic mutations? Proteins 2004;55:1–10.
10. Maegley KA, Admiraal SJ, Herschlag D. Ras-catalyzed hydrolysis of GTP: a new perspective from model studies. Proc Natl Acad Sci USA 1996;93:8160–8166.
11. Sprang SR. GAP into the breach. Science 1997;277:329–330.
12. Bourne HR. G proteins: the arginine finger strikes again. Nature 1997;389:673–674.
13. Vetter IR, Wittinghofer A. The guanine nucleotide-binding switch in three dimensions. Science 2001;294:299–1304.
14. Kosloff M, Selinger Z. Substrate assisted catalysis—application to G proteins. Trends Biochem Sci 2001;26:161–166.
15. Der CG, Finkel T, Cooper GM. Biological and biochemical properties of human ras^H genes mutated at codon 61. Cell 1986;44:167–176.
16. Futatsugi N, Hata M, Hoshino T, Tsuda M. Ab initio study of the role of lysine 16 for the molecular switching mechanism of ras protein p21. Biophys J 1999;77:3287–3292.
17. Katagiri D, Hata M, Itoh T, Neya S, Hoshino T. Atomic-scale mechanism of the GTP → GDP hydrolysis reaction by the Giα1 protein. J Phys Chem B 2003;107:3278–3283.
18. Resat H, Straatsma TP, Dixon DA, Miller JH. The arginine finger of RasGAP helps Gln-61align the nucleophilic water in GAP-stimulated hydrolysis of GTP. Proc Natl Acad Sci USA 2001;98:6033–6038.
19. Cavalli A, Carloni P. Enzymatic GTP hydrolysis: insights from an ab initio molecular dynamics. J Am Chem Soc 2002;124:3763–3768.
20. Topol IA, Cachau RE, Nemukhin AV, Grigorenko BL, Burt SK. Quantum chemical modeling of the GTP hydrolysis by the Ras-GAP protein complex. Biochem Biophys Acta 2004;1700:125–136.
21. Du X, Black GE, Lecchi P, Abramson FP, Sprang SR. Kinetic isotope effects in Ras-catalyzed GTP hydrolysis: evidence for a loose transition state. Proc Natl Acad Sci USA 2004;101:8858–8863.
22. Warshel A, Levitt M. Theoretical studies of enzymatic reactions: Dielectric, electrostatic, and steric stabilization of the carbonium ion in the reaction of lyzozyme. J Mol Biol 1976;103:227–249.
23. Field MJ, Bash PA, Karplus MA. Combined ab initio quantum mechanical and molecular mechanical method for carrying out simulations on complex molecular systems: applications to the $CH_3Cl + Cl^-$ exchange reaction and gas phase protonation of polyethers. J Comput Chem 1990;11:700–733.
24. Gao JL, Xia XF. A priori evaluation of aqueous polarization effects through Monte Carlo QM/MM simulations. Science 1992;258:631–635.
25. Nemukhin AV, Grigorenko BL, Bochenkova AV, Topol IA, Burt SK. A QM/MM approach with effective fragment potentials applied to the dipeptide-water structures. J Mol Struct (Theochem) 2002;581:167–175.
26. Grigorenko BL, Nemukhin AV, Topol IA, Burt SK. Modeling of

biomolecular systems with the quantum mechanical and molecular mechanical method based on the effective fragment potential technique: proposal of flexible fragments. J Phys Chem A 2002;106: 10663–10672.
27. Nemukhin AV, Grigorenko BL, Topol IA, Burt SK. Flexible effective fragment QM/MM method: validation through the challenging tests. J Comp Chem 2003;24:1410–1420.
28. Nemukhin AV, Grigorenko BL, Rogov AV, Topol IA, Burt SK. Modeling of the serine protease prototype reactions with the flexible effective fragment potential QM/MM method. Theor Chem Acc 2004;111:36–48.
29. Gordon MS, Freitag MA, Bandyopadhyay P, Jensen JH, Kairys V, Stevens WJ. The effective fragment potential method: a QM-based MM approach to modeling environmental effects in chemistry. J Phys Chem A 2002;105:293–307.
30. Schmidt MW, Baldridge KK, Boatz JA, Elbert ST, Gordon MS, Jensen JH, Koseki S, Matsunaga N, Nguyen KA, Su SJ, and others. The general atomic and molecular electronic structure system. J Comp Chem 1993;14:1347–1356.
31. Nemukhin AV, Grigorenko BL, Granovsky AA. Molecular modeling with the PC GAMESS system: from diatomic molecules to enzymes. Moscow State Univ Res Bull, Khimia 2004;45:75–102.
32. Ponder JW, Richards FM. An efficient Newton-like method for molecular mechanics energy minimization of large molecules. J Comput Chem 1987;8:1016–1026.
33. Danning TH, Hay PJ. In: Schaefer HF, editor. Methods of electronic structure theory, Vol 2. New York: Plenum Press; 1977.
34. Cornell WD, Cieplak P, Bayly CI, Gould IR, Merz KM, Ferguson DM, Spellmeyer DC, Fox T, Caldwell JW, Kollman PA. A second generation force field for the simulation of proteins, nuclear acids, and organic molecules. J Amer Chem Soc 1995;117:5179–5197.
35. Frisch MJ, Trucks GW, Schlegel HB, Scuseria GE, Robb MA, Cheeseman JR, Zakrzewski VG, Montgomery JA, Stratmann RE, Burant JC, and others. Gaussian98, A.1 ed., Pittsburg; 1998.
36. Feuerstein J, Goody RS, Webb MR. The mechanism of guanosine triphosphate hydrolysis by p21 c-Ha-ras. The stereochemical course of the GTPase reaction. J Biol Chem 1989;264:6188–6190.
37. Fu A, Li H, Du D, Zhou Z. Theoretical study on the reaction mechanism of proton transfer in formamide. Chem Phys Lett 2003;382:332–337.
38. Markova N, Enchev V. Water-assisted proton transfer in formamide, thioformamide and selenoformamide. J Mol Struct (Theochem) 2004;679:195–205.
39. Ahmadian MR, Stege P, Schffzek K, Wittinghofer A. Confirmation of the arginine-finger hypothesis for the GAP-stimulated GTP-hydrolysis reaction of Ras. Nat Struct Biol 1997;4:686–689.
40. Graham DL, Eccleston JF, Lowe PN. The conserved arginine in Rho-GTPase-activating protein is essential for efficient catalysis but nit for complex formation with Rho.GDP and aluminum fluoride. Biochemistry 1999;38:985–991.
41. Sondek J, Lambright DG, Noel JP, Hamm HE, Sigler PB. GTPase mechanism of Gproteins from the 1.7-Å crystal structure of transducin α GDP AlF_4^-. Nature 1994;372:276–279.
42. Nemukhin AV, Topol IA, Grigorenko BL, Burt SK. On the origin of potential barrier for the reaction $OH^- + CO_2 \rightarrow HCO_3^-$ in water: studies by using continuum and cluster salvation methods. J Phys Chem 2002;106:1734–1740.
43. Nemukhin AV, Grigorenko BL, Topol IA, Burt SK. QM/MM modeling of the glutathione-hydroxymethyl radical reaction in water. Phys Chem Chem Phys 2004; 6; 1031–1038.